

# Equation of state of supercooled water simulated using the extended simple point charge intermolecular potential

Stephen Harrington

Center for Polymer Studies and Department of Physics, Boston University, Boston, Massachusetts 02215

Peter H. Poole

Department of Applied Mathematics, University of Western Ontario, London, Ontario N6A 5B7, Canada

Francesco Sciortino

Dipartimento di Fisica and Istituto Nazionale per la Fisica della Materia, Universita' di Roma La Sapienza, Piazzale Aldo Moro 2, I-00185, Roma, Italy

H. Eugene Stanley

Center for Polymer Studies and Department of Physics, Boston University, Boston, Massachusetts 02215

(Received 14 July 1997; accepted 8 August 1997)

We carry out extensive molecular dynamics simulations in order to evaluate the thermodynamic equation of state of the extended simple point charge model of water (customarily described by the acronym SPC/E) over a wide range of temperature and density, with emphasis on the supercooled region. We thereby determine the location of the temperature of maximum density (TMD) line and the liquid spinodal line. In particular, we find that the experimental TMD line lies between the TMD lines of the SPC/E and ST2 models of water, so perhaps the behavior of these two models of simulated water "bracket" the behavior of real water. As temperature decreases, we find (i) that maxima appear in isotherms of the isothermal compressibility as a function of density, (ii) that isotherms of the internal energy as a function of volume display negative curvature and (iii) that the pressure of the liquid-vapor spinodal decreases. We compare the results to corresponding behavior found from simulations of the ST2 model of water and find that the behavior of SPC/E, when shifted to higher values of temperature and pressure ( $\Delta P \approx 50$  MPa and  $\Delta T \approx 80$  K), approximates that of ST2. We discuss the implications of our results for the hypothesis that a critical point occurs in the phase diagram of supercooled water. Finally, we argue that the results of our simulations are not inconsistent with the possibility that  $C'$  exists for SPC/E water. © 1997 American Institute of Physics. [S0021-9606(97)52242-2]

## I. INTRODUCTION

The supercooled state of liquid water and the mechanism that results in the anomalous behavior in thermodynamic response functions as temperature,  $T$ , decreases remains an open question in the study of network-forming liquids.<sup>1</sup> Recent experimental work, theoretical results and computer simulations have added substantially to the debate on the nature of supercooled water.<sup>2-9</sup> The current interpretations of apparent divergences in various functions describing supercooled water are categorized into three groups.<sup>2</sup> The stability limit conjecture (SLC) states that the divergences in thermodynamic response functions are due to the liquid-vapor spinodal that re-enters the positive pressure region of the phase diagram at low  $T$ .<sup>3</sup> The critical point hypothesis proposes a new critical point,  $C'$ , that is the terminus of the line of first order phase transitions between two low  $T$  liquid phases differing in density,  $\rho$ .<sup>4-6</sup> Critical fluctuations as  $T \rightarrow T_{C'}$  are responsible for the thermodynamic divergences. The singularity-free interpretation consists of the view that these increases in response functions attain maximum values, but remain finite for all  $T$ .<sup>7</sup>

Examples of experimental studies include thermodynamic<sup>1,9</sup> and transport<sup>10,11</sup> measurements as well as structural measurements using x-ray<sup>12</sup> and neutron

scattering.<sup>13</sup> Experiments are difficult to perform in the deeply supercooled region of the phase diagram, so simulations of models of water have contributed to understanding the thermodynamic behavior of the bulk liquid. Model potentials, whether rigid molecular models, polarizable potentials, or *ab initio* calculations only approximate the properties of water; comparison with known properties allows one to infer the accuracy of the model. Many rigid molecule potentials display qualitatively the same thermodynamic behavior as water, but disagree quantitatively, both with each other, and with experimental results on water.

Two rigid-molecule models of water that are widely studied are the ST2<sup>14</sup> and SPC/E<sup>15-18</sup> models. The ST2 model places oppositely charged pairs at the corners of a tetrahedron about the center of mass. ST2 is *over-structured* compared to water and the equation of state is shifted to higher values of pressure,  $P$ , and  $T$ . The SPC/E model has three point charges, located at the atomic centers of the water molecule. SPC/E is *under-structured* with its equation of state shifted to lower values of pressure,  $P$ , and  $T$  as we show below. Also, at the same  $T$  and  $P$ , ST2 molecules are more mobile compared to real water, while SPC/E is less mobile. Thus it may be possible that the ST2 and SPC/E models bracket the thermodynamic behavior of water in the  $PT$  plane. A third rigid-molecule model of water widely

used is the TIP4P model,<sup>19</sup> that is similar to the SPC/E model.

SPC/E is one of the most commonly used rigid-molecule pair potential models for water, both for the study of pure liquid water as well as for simulations of water near solute molecules and extended surfaces. The SPC/E potential has been explicitly parametrized to reproduce the experimental value of the self-diffusion constant at ambient temperature,  $T=298$  K and density,  $\rho=1$  g/cm<sup>3</sup> and it has been widely studied in recent years.<sup>16,17</sup> A temperature of maximum density (TMD) has been found along the 1 g/cm<sup>3</sup> isochore<sup>4</sup> and at ambient pressure.<sup>18</sup> The temperature dependence of dynamical quantities at low and negative pressures have also been studied.<sup>8,18</sup> However, most studies using SPC/E water have been conducted for a relatively small number of thermodynamic states. A comprehensive knowledge of the behavior of the SPC/E model over a wide range of  $T$ ,  $\rho$  and  $P$  is lacking, especially at low  $T$ . As well, the  $P$ -dependence of the TMD line in SPC/E is not known.

Studies employing the ST2 and TIP4P potentials suggest that in addition to the known critical point  $C$  at temperature  $T_C=647$  K, pressure  $P_C=22.8$  MPa, and density  $\rho_C=0.326$  g/cm<sup>3</sup>, a *second* critical point  $C'$  might possibly occur at low  $T$ .<sup>4,20</sup> Indeed, conclusive evidence for coexisting liquid phases for  $T<T_{C'}$  has been found in recent simulations using the ST2 potential.<sup>6</sup> Moreover, an interrelated set of novel thermodynamic behavior—in particular, maxima in isotherms of the isothermal compressibility  $K_T$  as a function of density and a change in the slope of the TMD line in the  $P$ - $T$ -plane—are found in both ST2 and TIP4P simulations for  $T$  greater than the proposed critical temperature,  $T_{C'}$ .<sup>5</sup> This behavior can be interpreted as thermodynamic precursors of the phase separation that occurs for  $T<T_{C'}$ .<sup>7</sup> Knowledge of the behavior of SPC/E at low  $T$  could, in particular, further test the hypothesis that a critical point and liquid–liquid phase transition occurs.

In the present work, we perform molecular dynamics (MD) simulations to evaluate the thermodynamic properties of the SPC/E model in the region of the supercooled liquid.<sup>21</sup> The results provide an overall picture of the low  $T$  equation of state of SPC/E, permitting a comparison both with real water and other simulation potentials. We specifically test SPC/E for the novel thermodynamic behavior found in simulations of TIP4P and ST2. Since the ST2 potential overestimates the structure in liquid water, we choose to study the SPC/E potential that under-estimates the structure in liquid water.<sup>22</sup> We find that the SPC/E model displays (i) a TMD line that changes slope at negative pressures, (ii) a maxima in the isothermal compressibility as a function of the density and (iii) a monotonically decreasing spinodal. However, we are unable to perform simulations at the value of  $T_{C'}$  we estimate for SPC/E as the time required for equilibration is prohibitively long.

## II. METHOD

We employ the  $(N, V, T)$  ensemble ( $V$  is the volume and  $N=216$  is the number of molecules). We start the simulation

by melting a cubic ice configuration at 600 K and then lowering  $T$  to 340 K, using a Berendsen rescaling of the velocities with a relaxation time of 1 ps at the highest  $T$  and 50 ps at the lowest  $T$ .<sup>23</sup> We approximate the effect of the long-range Coulombic interactions using the reaction field method with a cutoff of 0.78 nm. We solve the equations of motion using a velocity Verlet update with time step of 1 fs.<sup>24–26</sup>

We perform simulations of 7 to 8 independent runs for each state point (see Table I). We start the equilibration runs at low  $T$  from preexisting equilibrated configurations with the same density but at 10 K higher  $T$ . We lower  $T$  by rescaling the velocities in the same manner as described above. We allow the system to equilibrate for 500 ps at the highest  $T$  and 10 ns at the lowest  $T$ . We confirm that equilibrium is attained when quantities such as  $P$  or potential energy fluctuate about some average value that is independent of the time interval sampled. In addition, we find that the distributions of  $P$  and the configurational part of the internal energy,  $U$ , are the same for each independent run at the same state point, approximating a Gaussian distribution around the average value. We also confirm that, at long times, the mean square displacement,  $\langle r^2(t) \rangle$ , depends linearly on  $t$  and that  $\langle r^2 \rangle$  attains a value greater than one molecular diameter ( $\approx 0.3$  nm) over the course of the equilibration period. For each state point  $(T, \rho)$ , we calculate a running average of  $P$  and  $U$  for the system every 0.1 ps after equilibration. To provide an estimate of the computational effort involved in this research, we note that the simulation time for all state points recorded in Table I is  $\approx 3.6$   $\mu$ s. We obtain simulation speeds of  $\approx 60$   $\mu$ s/particle update, for a total of 1600 CPU days of computation (three months total time, since we use an average of 16 processors in parallel).

## III. TMD LINE AND SPINODAL LINE

To investigate the behavior of the TMD line, we show in Fig. 1a constant volume isochores of  $P$  as a function of  $T$ . The locus of minima occurring in the isochores locates the position of the TMD line.<sup>4</sup> We present in Fig. 1b a set of graphs using different scales for each isochore. Note that a minimum exists for each isochore in the range  $1.10 > \rho > 0.95$  g/cm<sup>3</sup>. The TMD line thus obtained is shown in Fig. 2a, and compared with that of ST2 and the experimental results for water. We find, as for ST2, that the slope in the  $P$ - $T$  plane of the TMD line for SPC/E changes sign from negative to positive as  $P$  decreases into the region of the stretched liquid at  $P < 0$ . The relative shift between the TMD line for SPC/E and ST2 is estimated to be  $\Delta P \approx 50$  MPa and  $\Delta T \approx 80$  K, with SPC/E shifted to lower values of  $P$  and  $T$  relative to ST2. For water, experiments at  $P < 0$  have not located the TMD line, hence the change in the slope of the TMD line (the “nose”) is not known. Although metastable water under high negative pressures has been experimentally produced<sup>27</sup> (up to  $-200$  MPa) and studied spectroscopically, density measurements under such conditions have not been accomplished and remain one of the challenging tasks for future experiments.

The lowest density isochore of  $P$  versus  $T$

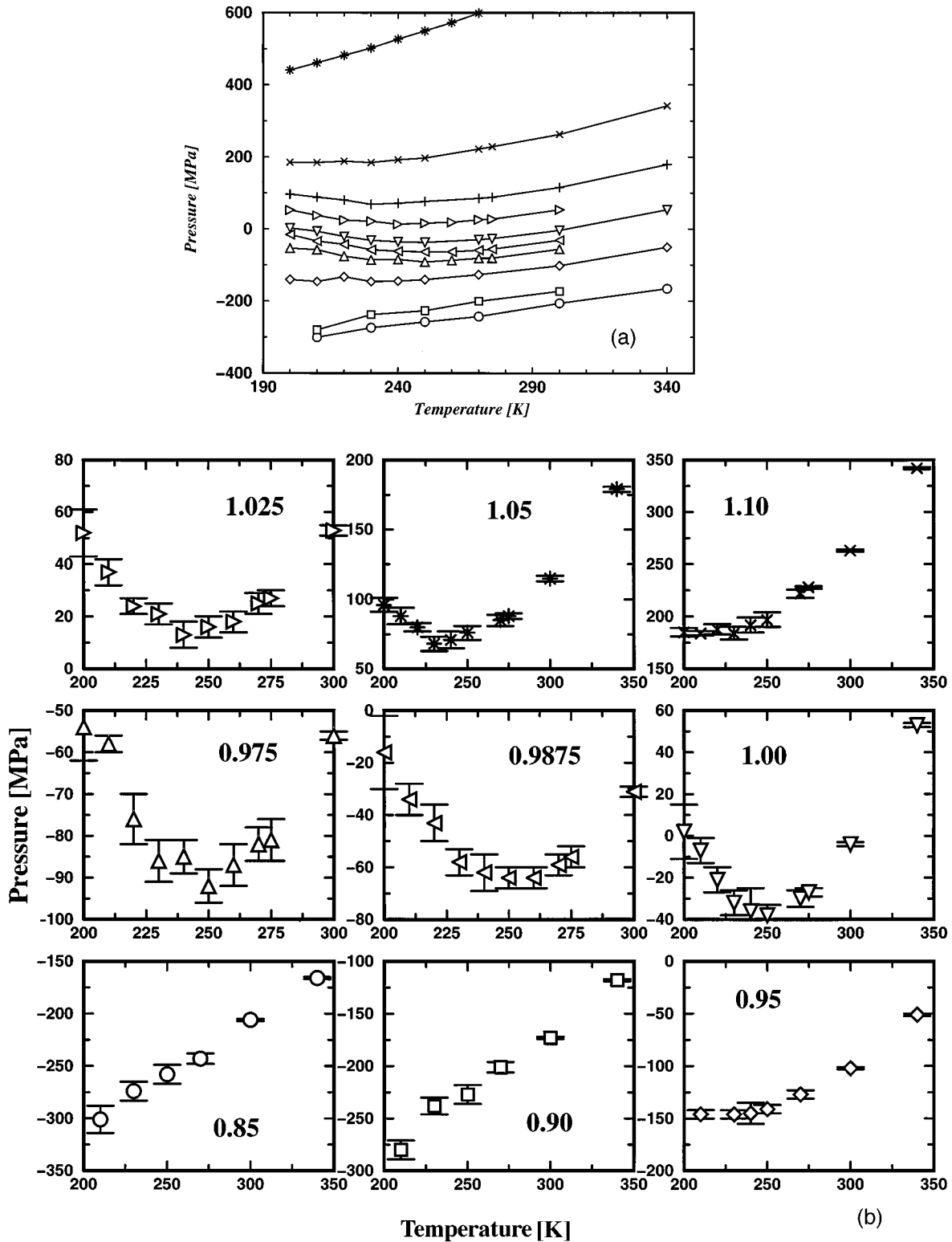


FIG. 1. SPC/E equation of state. (a) Isochores of  $P(T)$  for  $\rho=0.85$  to  $\rho=1.20$   $\text{g}/\text{cm}^3$  for  $200 \leq T \leq 340$  K. From top to bottom,  $\rho=1.20, 1.10, 1.05, 1.025, 1.00, 0.9875, 0.975, 0.95, 0.90, 0.85$   $\text{g}/\text{cm}^3$ . (b) Detail of each isochore for  $0.85 < \rho < 1.10$   $\text{g}/\text{cm}^3$ . Error bars for  $P$  represent the statistical uncertainty and are calculated from averages over typically 8 independent samples (see Table I). Note the minima,  $(\partial P / \partial T)_V = 0$ , for  $0.975 \leq \rho \leq 1.05$ .

( $\rho=0.85$   $\text{g}/\text{cm}^3$ ) places an upper bound on the location of the liquid spinodal, the metastability limit at which the (stretched) liquid phase cavitates to form the vapor phase. The monotonic decrease of  $P$  along an isochore as  $T$  de-

creases for  $\rho < 0.90$   $\text{g}/\text{cm}^3$  indicates that the TMD line does not intersect the liquid spinodal in the region of our simulations. Our results therefore suggest that, like the ST2 model, the SPC/E model exhibits a monotonic spinodal line in the

TABLE I. Results for simulated state points of the SPC/E model for a system of size  $N=216$  molecules.  $U$  is the configurational part of the internal energy,  $D$  the diffusivity and  $t_{\text{run}}$  is the total run time. All values are averaged over 7 to 8 independent runs. The statistical error for  $U$  is less than 0.03 kJ/mol for all state points.

$T$ (K)	$\rho$ (g/cm <sup>3</sup> )	$P$ (MPa)	$U$ (kJ/mol)	$t_{\text{run}}$ (ns)
200	0.975	-54±8	-54.27	30
200	0.9875	-16±14	-54.30	30
200	1.00	2±13	-54.15	30
200	1.025	52±9	-54.15	30
200	1.05	96±5	-54.03	30
200	1.10	185±4	-53.89	30
200	1.20	441±5	-53.81	30
210	0.85	-301±13	-52.07	2
210	0.90	-280±9	-52.82	2
210	0.95	-146±4	-53.21	2
210	0.975	-58±2	-53.45	10
210	0.9875	-34±6	-53.53	10
210	1.00	-7±6	-53.47	10
210	1.025	37±5	-53.40	10
210	1.05	88±6	-53.32	10
210	1.10	184±2	-53.20	10
210	1.20	461±4	-53.18	10
210	1.40	1629±4	-52.84	10
210	1.50	2885±4	-51.87	10
220	0.975	-76±6	-52.65	5
220	0.9875	-43±7	-52.76	5
220	1.00	-21±6	-52.66	5
220	1.025	24±3	-52.67	5
220	1.05	80±3	-52.62	5
220	1.10	188±5	-52.48	5
220	1.20	482±4	-52.48	5
220	1.40	1726±4	-52.33	5
220	1.50	2937±4	-51.52	5
230	0.85	-274±9	-50.53	1
230	0.90	-238±8	-51.10	1
230	0.95	-146±4	-51.82	1
230	0.975	-86±5	-51.87	5
230	0.9875	-58±5	-51.91	5
230	1.00	-32±6	-51.90	5
230	1.025	24±4	-51.89	5
230	1.05	68±5	-51.90	5
230	1.10	184±6	-51.85	5
230	1.20	502±4	-51.84	5
230	1.40	1779±4	-51.62	5
230	1.50	2972±4	-51.10	5
240	0.95	-145±10	-51.00	1
240	0.975	-85±4	-51.16	1
240	0.9875	-62±7	-51.19	1
240	1.00	-36±11	-51.18	1
240	1.025	13±3	-51.17	1
240	1.05	71±6	-51.19	1
240	1.10	192±7	-51.21	1
240	1.20	527±5	-51.26	1
240	1.40	1863±5	-50.98	1
240	1.50	3044±5	-50.65	1
250	0.85	-258±9	-49.05	1
250	0.90	-227±9	-49.79	1
250	0.95	-141±4	-50.22	1
250	0.975	-92±4	-50.37	1
250	0.9875	-64±4	-50.40	1
250	1.00	-38±5	-50.44	1
250	1.025	16±5	-50.49	1
250	1.05	76±5	-50.54	1
250	1.10	197±7	-50.55	1
250	1.20	550±5	-50.64	1
250	1.40	-1927±4	-50.40	1

TABLE I. (Continued.)

$T$ (K)	$\rho$ (g/cm <sup>3</sup> )	$P$ (MPa)	$U$ (kJ/mol)	$t_{\text{run}}$ (ns)
250	1.50	3149±5	-49.80	1
260	0.975	-87±5	-49.64	1
260	0.9875	-64±4	-49.69	1
260	1.025	18±4	-49.78	1
260	1.20	573±4	-50.09	1
260	1.40	1980±4	-49.84	1
260	1.50	3257±4	-49.22	1
270	0.85	-243±4	-47.46	1
270	0.90	-201±5	-48.18	1
270	0.95	-127±4	-48.69	1
270	0.975	-82±4	-48.89	1
270	0.9875	-59±4	-48.97	1
270	1.00	-30±5	-49.02	1
270	1.025	25±3	-49.13	1
270	1.05	85±4	-49.23	1
270	1.10	222±4	-49.38	1
270	1.20	599±4	-49.51	1
270	1.30	1185±5	-49.51	1
270	1.40	2061±5	-49.23	1
270	1.50	3356±5	-48.63	1
275	0.975	-81±5	-48.58	0.5
275	0.9875	-56±4	-48.68	0.5
275	1.00	-27±2	-48.72	0.5
275	1.025	27±3	-48.84	0.5
275	1.05	88±2	-48.92	0.5
275	1.10	228±1	-49.09	0.5
300	0.85	-206±1	-45.4	0.5
300	0.90	-173±1	-46.0	0.5
300	0.95	-102±1	-46.6	0.5
300	0.975	-56±1	-46.93	0.5
300	0.9875	-31±2	-47.00	0.5
300	1.00	-4±1	-47.11	0.5
300	1.025	53±2	-47.28	0.5
300	1.05	115±2	-47.42	0.5
300	1.10	263±1	-47.66	0.5
340	0.85	-166±1	-43.0	0.5
340	0.90	-118±1	-43.7	0.5
340	0.95	-51±1	-44.3	0.5
340	1.00	53±1	-44.9	0.5
340	1.05	179±2	-45.3	0.5
340	1.10	342±1	-45.6	0.5

$P$ - $T$  plane rather than re-entrant spinodal.<sup>3</sup> The spinodal line decreases monotonically and avoids intersecting the TMD.

#### IV. $P$ - $\rho$ ISOTHERMS AND THE ISOTHERMAL COMPRESSIBILITY

For ST2 inflections in isotherms of  $P$  as a function of  $\rho$  have been found that evolve as  $T$  decreases to give a critical isotherm for  $T=T_{C'}$ , followed at lower  $T$  by doubled-branched isotherms bracketing a region of first-order phase coexistence.<sup>6</sup> For SPC/E, we show in Fig. 3 the corresponding  $T=250, 230,$  and  $200$  K isotherms. We find that an inflection appears in the isotherms for  $T<250$  K between  $\rho=0.975$  g/cm<sup>3</sup> and  $\rho=1.025$  g/cm<sup>3</sup>. We can use the shift in  $T$ ,  $\Delta T\approx 80$  K, between the TMD lines of ST2 and SPC/E to estimate the possible location of  $C'$  for SPC/E. If SPC/E behaves similarly to ST2, its  $C'$  should be observable around

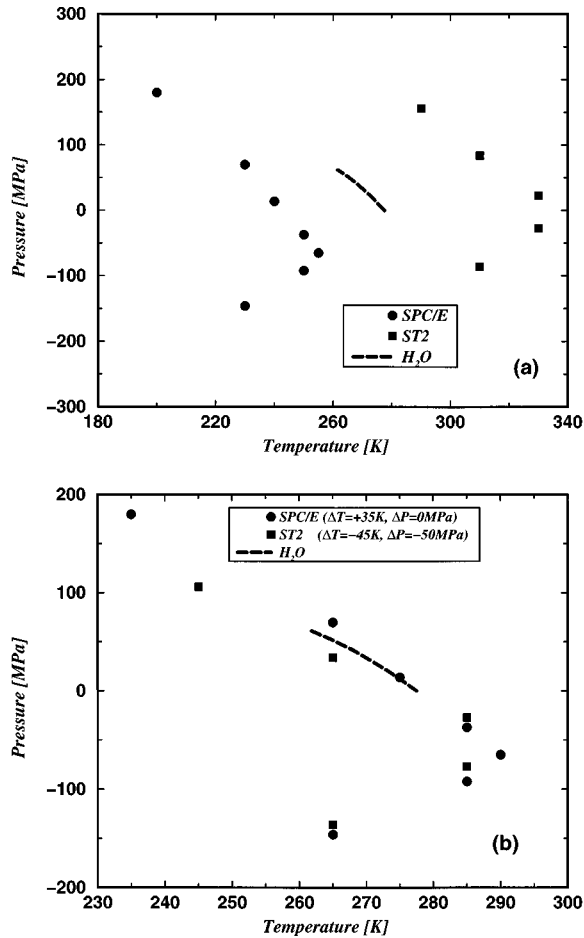


FIG. 2. (a) The temperature of maximum density (TMD) line for the ST2 (filled squares) and the SPC/E (filled circles) models, as determined from the isochores of  $P(T)$ . The maximum occurs at  $T \approx 330$  K and  $P \approx 0$  MPa for the ST2 model and  $T \approx 250$  K at  $P \approx -50$  MPa for the SPC/E model. (b) TMD lines for ST2, SPC/E and water.  $T$  for SPC/E has been shifted by  $+35$  K and for ST2 by  $-45$  K. The ST2 TMD line has also been shifted in pressure  $-50$  MPa. Note the close correspondence to the experimental TMD.

$$T_{C'}(\text{SPC/E}) = T_{C'}(\text{ST2}) - \Delta T \approx 160 \text{ K}, \quad (4.1)$$

a temperature at which we are not able to perform equilibrium simulations. Indeed, in the range of  $T$  in which we are able to conduct simulations, a critical isotherm does not occur for SPC/E. Hence if  $C'$  does occur in the phase diagram of SPC/E, it must be the case that  $T_{C'}$  is less than the lowest  $T$  simulated in this work, i.e.  $T_{C'} < 200$  K.

We next calculate  $K_T$  from the  $P$ - $\rho$  isotherms of Fig. 3. We perform a sixth-order polynomial fit to the  $P\rho$  data and a numerical differentiation  $\rho^{-1}(\partial\rho/\partial P)_T$  to estimate  $K_T$ . In Fig. 4,  $K_T$  is plotted as a function of  $\rho$ . We note two interesting features: (i) A maximum in  $K_T$  occurs for each of the low  $T$  isotherms, and (ii) the value of  $K_T$  at its maximum,  $K_T^{\max}$ , increases on cooling. The ‘‘line of  $K_T$  maxima’’ is shown in Fig. 5, along with the TMD line and an upper bound on the spinodal.

A study of  $K_T$  for the ST2 potential has been reported elsewhere,<sup>5</sup> and the behavior of  $K_T^{-1}$  was used to locate  $C'$  at  $T_{C'} \approx 235$  K,  $P_{C'} \approx 200$  MPa and  $\rho_{C'} \approx 1.00$  g/cm<sup>3</sup>. Since

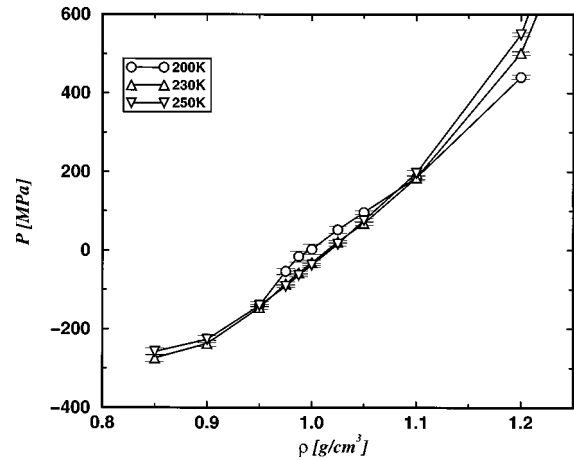


FIG. 3. Isotherms of  $P(\rho)$  for  $T=250$  K (down triangle),  $T=230$  K (up triangle),  $T=200$  K (circle). Note the inflection at  $T=200$  K.

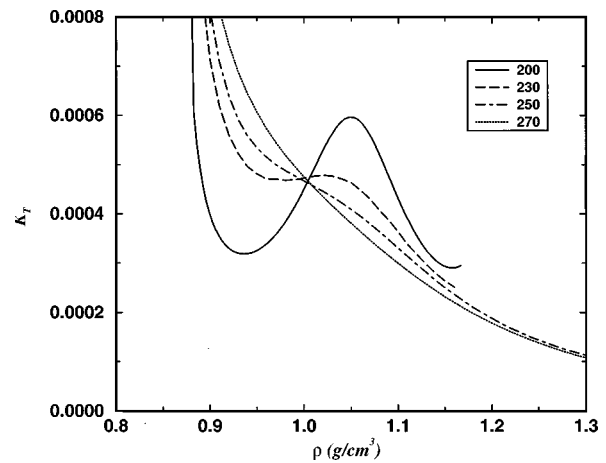


FIG. 4. Isothermal compressibility,  $K_T$ , as a function of density evaluated from a sixth-order polynomial fit of the isotherms in Fig. 3. Note that  $K_T$  displays a maximum for  $T < 250$  K at  $\rho > 1.00$  g/cm<sup>3</sup>.

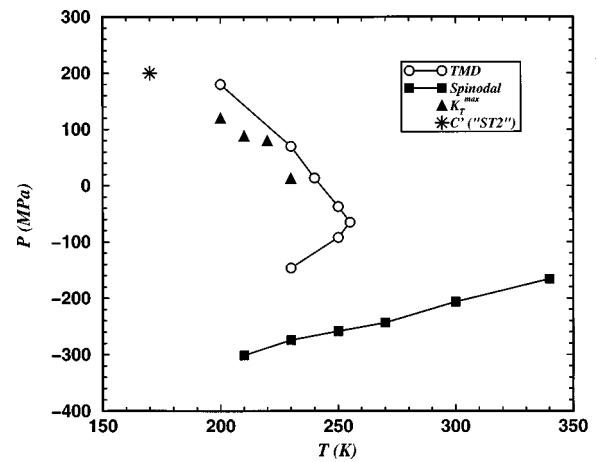


FIG. 5. The TMD line (open circles) is determined from the minima in each of the isochores of  $P(T)$  (Fig. 1b). The location of the maxima of  $K_T(V)$  in Fig. 4 are shown as filled triangles. The spinodal line (filled squares) is estimated from the  $0.85$  g/cm<sup>3</sup> isochore of Fig. 1b. The ‘‘star’’ denotes where  $C'$  would be for the ST2 coordinates shifted in  $T$  and  $P$  by  $80$  K and  $50$  MPa, respectively. Note that the TMD line changes slope for  $P < -80$  MPa and that the line of  $K_T$  maxima is negatively sloped.

the lowest value of  $T$  that we simulated in the SPC/E model is much larger than  $T_{C'}$ , we cannot use the same analysis to locate the coordinates of  $C'$ . However, applying the relative shift in the TMD between ST2 and SPC/E suggests that  $K_T$  might diverge at  $T_{C'}(\text{SPC/E}) \approx 160$  K and  $P_{C'}(\text{SPC/E}) \approx 200$  MPa. From Fig. 4, the maximum in  $K_T$  is increasing near  $\rho \approx 1.05$  g/cm<sup>3</sup>, so that we estimate  $\rho_{C'}(\text{SPC/E}) \approx 1.07$  g/cm<sup>3</sup>.

## V. INTERNAL ENERGY

The configurational part of the internal energy,  $U$ , is related to the configurational Helmholtz free energy  $A = U - TS$ , where  $S$  is the configurational entropy. Differentiating  $A$  twice with respect to  $V$  and using the fact that  $P = -(\partial A / \partial V)_T$ , we obtain  $K_T^{-1} = V[(\partial^2 U / \partial V^2)_T - T(\partial^2 S / \partial V^2)_T]$ . The curvature of an isotherm in  $A$  must be greater than zero for a given density to be thermodynamically stable.<sup>28</sup> Hence,  $K_T$  can be decomposed into two parts: One due to the isothermal dependence of  $U$  on  $\rho$ , and one due to the dependence of  $S$  on  $\rho$ .

The contribution of  $U$  to the thermodynamic stability of liquid can be studied directly using the present data. In Fig. 6a, isotherms of  $U(V)$  are shown. Note the increase in  $U$  at high and low densities. At low densities (high  $V$ ) the system approaches its limit of mechanical stability and so  $U$  increases. At high densities (small  $V$ ) the molecules are experiencing the  $r^{-12}$  repulsive potential of the Lennard-Jones term of the intermolecular pair potential. For the highest  $T$ ,  $U$  is a positively curved (i.e. concave-upward) function of  $\rho$  between these limits. However, isotherms for  $T < 240$  K display a region of negative curvature within these two limits. In this region the contribution of  $U$  is to reduce  $K_T$  and the liquid is stable due only to a positive contribution from the behavior of  $S$ . Similar behavior for  $U$  has been found for ST2. In Fig. 6b, the  $T = 210$  K isotherm is shown on an increased scale. Note the region of negative curvature that develops. At high  $T$ , isotherms of  $U(V)$  display a smooth continuous curvature between the hard core repulsive potential at small  $V$  and the spinodal at high  $V$ . At  $T = 230$  K and below, a region of negative curvature develops starting near  $V \approx 1.0$  cm<sup>3</sup>/g and extending to smaller  $V$ .

## VI. DISCUSSION

In this article, we report MD simulation results concerning the evaluation of the thermodynamic properties of the SPC/E potential in the supercooled and stretched states. We calculate the line in the  $PT$ -plane along which the density has an isobaric maximum and find that the TMD line presents a nose at negative pressure. The presence of the TMD line in the phase diagram as well as its shape is particularly relevant, because the TMD line acts as a ‘‘thermodynamic constraint’’ for the temperature dependence of several other thermodynamic quantities. For example, the fact that the TMD line has a nose in the  $P-T$  plane implies that the liquid-gas spinodal is not re-entrant. Indeed, we also calculate an upper bound limit for the spinodal line, i.e. the line along which the liquid phase loses its stability with respect to

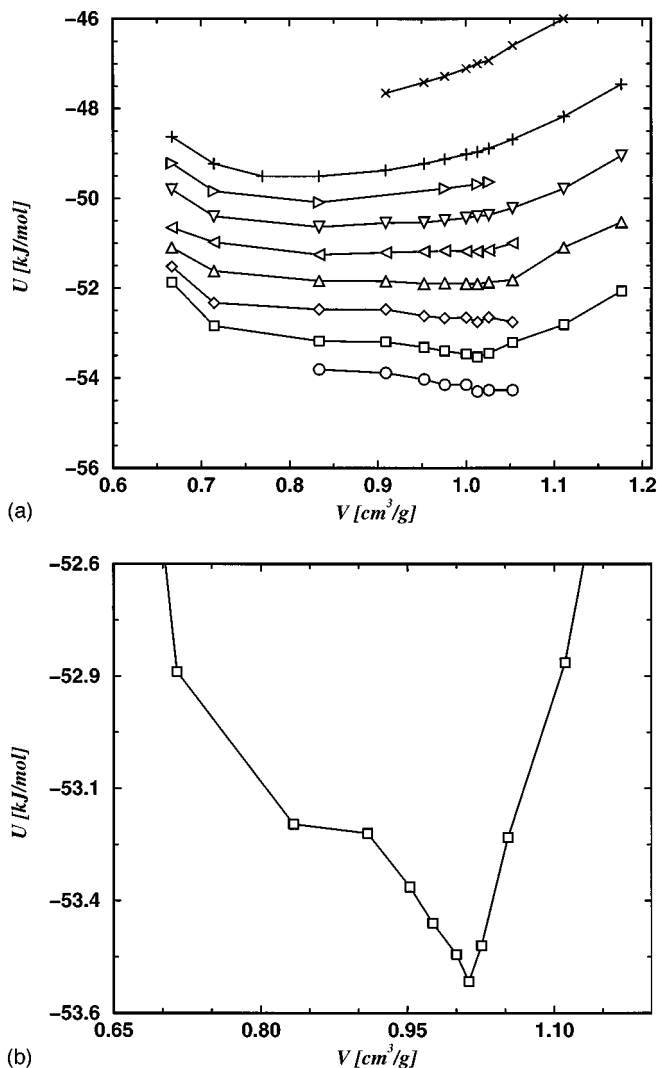


FIG. 6. (a) Isotherms  $U(V)$  for  $T = 200$  K (circle), 210 K (square), 220 K (diamond), 230 K (up triangle), 240 K (left triangle), 250 K (down triangle), 260 K (right triangle), 270 K (plus), 300 (×), and 340 K (star). The statistical error is typically less than 0.03 kJ/mol for all state points, smaller than the symbol size. (b) Detail of  $T = 210$  K isotherm. Note the region of negative curvature near  $V \approx 0.90$  cm<sup>3</sup>/g.

gas-like fluctuations, and we show that such a line in the  $P-T$  plane monotonically decreases on cooling. Thus, as shown in Fig. 5, the TMD line does not intersect the spinodal line.

Another important constraint related to the presence and shape of the TMD line is the thermodynamic requirement of the presence in the phase diagram of a line of compressibility extrema. Reference 7 shows that along a constant pressure line crossing the TMD line in a point where  $(dP/dT)_{TMD} < 0$ , an isobar of  $K_T$  as a function of  $T$  must present a minimum for  $T > TMD$  and a maximum or a divergence for  $T < TMD$ . The line of states in the  $P-T$  plane along which such an extremum occurs is the ‘‘temperature of extremal compressibility’’ (TEC) line. The line of  $K_T$  maxima found in the present work (and also in Ref. 5) is defined as the line of states in the  $P-T$  plane at which an isotherm of  $K_T$  exhibits a maximum as a function of  $\rho$ . The

line of  $K_T$  maxima is thus distinct from the TEC line, but related to it, the two lines arising simply from different ways of “slicing” the  $K_T(T,P)$  surface, or equivalently, the  $K_T(T,\rho)$  surface. In water at ambient pressure, a point on the TEC line (specifically, a minimum of  $K_T$  as a function of  $T$  at constant  $P$ ) occurs at  $T=319$  K. Below  $T=319$  K, along an isobar  $K_T$  increases as  $T$  decreases in the experimentally accessible window (down to  $T=235$  K). We have shown here that in the case of SPC/E that a line of  $K_T$  maxima is observed in the supercooled regime, and we have calculated its position in  $P$ - $T$  plane.

The resulting phase diagram of SPC/E water is equivalent to that of ST2 water, another well-studied rigid pair-wise additive potential. In the case of SPC/E the charges are distributed only on the oxygen and hydrogen atoms, while in the case of ST2, charges are distributed on a tetrahedral structure. Although the positions of the TMD lines in the  $P$ - $T$ -plane are different, both their shape and their relative location are similar. In Fig. 2b, we show the simulation results for SPC/E and ST2 compared with the available thermodynamic data for water, to highlight the ability of these potentials to describe the thermodynamics of the real system. Curves for SPC/E and ST2 have been shifted in the  $PT$ -plane by the amounts discussed above, that maximizes the overlap with the experimental quantities. Compared to water, ST2 is over-structured, i.e. the formation of the hydrogen bonded network (the microscopic driving force that produces the density maximum anomalies) occurs at higher  $T$  compared to real water, so that the equation of state is shifted to higher values of  $T$  and  $P$ . In SPC/E water, the opposite behavior is observed, suggesting that SPC/E is under-structured compared to real water.

The SPC/E potential in the region accessible to the numerical simulations (i.e. in the region where equilibration times do not exceed 10 ns) behaves similarly to ST2. This similarity extends also to other thermodynamic quantities, as we show for  $\partial^2 U/\partial V^2$ . In the case of ST2, the higher relative  $T$  and  $P$  allows equilibrated simulations in a larger region of phase space, and permits the line of  $K_T$  maxima to be followed locating the critical point  $C'$ , below which a first-order liquid-liquid transition occurs. The reduced diffusivity of SPC/E compared to ST2 makes it impossible to study the low  $T$  and high  $P$  region, where the SPC/E second critical point should be located. Hence, we do not directly observe the occurrence of  $C'$ , but our results are not inconsistent with the possibility that  $C'$  exists for SPC/E water.

Both SPC/E and ST2 are models for describing the properties of water. As seen in Fig. 2b, and from the body of knowledge arising from more than 25 years of computer studies of water, the basic features of water are captured by the effective potential models used in the computer simulations. In this sense, ST2 and SPC/E are seen to describe a thermodynamic behavior that is similar to that of real water, although for different values of  $P$  and  $T$ . As we argue above, ST2 and SPC/E bracket the behavior of the real liquid, strongly suggesting that the study of these two potentials in a region of phase space not accessible to real experiments is relevant for understanding the thermodynamic behavior of

the real system. The similarity between SPC/E and ST2 and their ability to bracket the properties of real water support the possibility that in the experimentally inaccessible region, below the homogeneous nucleation temperature, water may undergo a liquid-liquid phase transition. The two distinct liquids generated below  $C'$  would be the reference liquids for the two observed amorphous form of water, low density amorphous (LDA) and high density amorphous (HDA) ice.<sup>29-31</sup>

## ACKNOWLEDGMENTS

We would like to thank S. Havlin and an anonymous referee for critical comments. on the manuscript. S.H. is supported by an NIH predoctoral training fellowship. P.H.P. acknowledges the support of NSERC (Canada). The Center for Polymer Studies is supported by the NSF and British Petroleum.

<sup>1</sup>For reviews, see P. G. Debenedetti, *Metastable Liquids* (Princeton University Press, Princeton, New Jersey 1997); C. A. Angell, *Science* **267**, 1924 (1995).

<sup>2</sup>F. Sciortino, in *Proceedings of the International School of Physics ‘‘Enrico Fermi’’*, Course CXXXIV, edited by F. Mallamace and H. E. Stanley (IOS Press, Amsterdam, 1997); P. H. Poole, T. Grande, C. A. Angell, and P. F. McMillan, *Science* **275**, 322 (1997); H. E. Stanley, L. Cruz, S. T. Harrington, P. H. Poole, S. Sastry, F. Sciortino, F. W. Starr, and R. Zhang, *Physica A* **236**, 19 (1997).

<sup>3</sup>R. J. Speedy, *J. Phys. Chem.* **86**, 982, 3002 (1982).

<sup>4</sup>P. H. Poole, F. Sciortino, U. Essmann, and H. E. Stanley, *Nature* **360**, 324 (1992); *Phys. Rev. E* **48**, 3799 (1993).

<sup>5</sup>F. Sciortino, P. H. Poole, U. Essmann, and H. E. Stanley, *Phys. Rev. E* **55**, 727 (1997).

<sup>6</sup>S. Harrington, R. Zhang, P. H. Poole, F. Sciortino, and H. E. Stanley, *Phys. Rev. Lett.* **78**, 2409 (1997).

<sup>7</sup>S. Sastry, P. G. Debenedetti, F. Sciortino, and H. E. Stanley, *Phys. Rev. E* **53**, 6144 (1996).

<sup>8</sup>P. Gallo, F. Sciortino, P. Tartaglia, and S.-H. Chen, *Phys. Rev. Lett.* **76**, 2730 (1996); F. Sciortino, P. Gallo, P. Tartaglia, and S.-H. Chen, *Phys. Rev. E* **54**, 6331 (1996).

<sup>9</sup>See, e.g., H. Kanno and C. A. Angell, *J. Chem. Phys.* **70**, 4008 (1979); C. A. Angell, in *Water: A Comprehensive Treatise*, edited by F. Franks (Plenum, New York 1972), Vol. 7.

<sup>10</sup>E. W. Lang and H.-D. Lüdemann, *Ber. Bunsenges. Phys. Chem.* **85**, 603 (1981).

<sup>11</sup>F. X. Prielmeier, E. W. Lang, R. J. Speedy, and H.-D. Lüdemann, *Phys. Rev. Lett.* **59**, 1128 (1987).

<sup>12</sup>Y. Xie, K. F. Ludwig, Jr., G. Morales, D. E. Hare, and C. M. Sorensen, *Phys. Rev. Lett.* **71**, 2050 (1993); L. Bosio, J. Teixeira, and H. E. Stanley, *ibid.* **46**, 597 (1981).

<sup>13</sup>M.-C. Bellissent-Funel and L. Bosio, *J. Chem. Phys.* **102**, 3727 (1995).

<sup>14</sup>F. H. Stillinger and A. Rahman, *J. Chem. Phys.* **60**, 1545 (1974).

<sup>15</sup>H. J. C. Berendsen, J. R. Grigera, and T. P. Straatsma, *J. Phys. Chem.* **91**, 6269 (1987).

<sup>16</sup>Y. Guissani and B. Guillot, *J. Chem. Phys.* **98**, 8221 (1993).

<sup>17</sup>P. E. Smith and W. F. van Gusteren, *Chem. Phys. Lett.* **215**, 315 (1993).

<sup>18</sup>L. A. Baez and P. Clancy, *J. Chem. Phys.* **101**, 9837 (1994); Note that Baez and Clancy find at 1 bar a temperature of maximum density  $T=253$  K, while we obtain about 242 K, a reasonable agreement considering that no long-range interaction is accounted for in the Baez-Clancy work.

<sup>19</sup>W. L. Jorgensen, J. Chandrasekhar, J. Madura, R. W. Impey, and M. Klein, *J. Chem. Phys.* **79**, 926 (1983).

<sup>20</sup>H. Tanaka, *Nature* **380**, 328 (1996); *J. Chem. Phys.* **105**, 5099 (1996).

<sup>21</sup>In the present work we use the word supercooled to refer to the range of  $T$  in which water is supercooled with respect to the crystalline state

- ( $T < 273$  K at atmospheric pressure). In fact, SPC/E does not display an ice  $I_h$  - liquid coexistence for  $T > 200$  K at  $P = 1$  atm (Ref. 18). However, liquid SPC/E is supercooled with respect to ice  $A$ , a form of crystalline ice not found in nature, for  $T < 295$  K at  $P = 1$  atm.
- <sup>22</sup>More precisely, SPC/E underestimates the effect of the local molecular structure on the thermodynamic properties of the liquid. Indeed, the oxygen pair correlation function of SPC/E has a sharper first peak at ambient and  $T$  compared to real water, yet the TMD line occurs at lower  $T$  for SPC/E. Hence, the impact of the structured network of hydrogen bonds on thermodynamic behavior is underestimated by SPC/E.
- <sup>23</sup>H. J. C. Berendsen, J. P. M. Postma, W. F. Van Gunsteren, A. Dinola, and J. R. Haak, *J. Chem. Phys.* **81**, 3684 (1984).
- <sup>24</sup>O. Steinhauser, *Mol. Phys.* **45**, 335 (1982).
- <sup>25</sup>M. P. Allen and D. J. Tildesley, *Computer Simulation of Liquids* (Oxford University Press, Oxford, 1989).
- <sup>26</sup>F. Sciortino, A. Geiger, and H. E. Stanley, *Phys. Rev. Lett.* **65**, 3452 (1990); *Nature* **354**, 218 (1991); *J. Chem. Phys.* **96**, 3857 (1992).
- <sup>27</sup>J. L. Green, D. J. Durben, G. H. Wolf, and C. A. Angell, *Science* **249**, 649 (1990).
- <sup>28</sup>H. E. Stanley, *Introduction to Phase Transitions and Critical Phenomena* (Oxford University Press, Oxford, 1971).
- <sup>29</sup>O. Mishima, L. D. Calvert, and E. Whalley, *Nature* **314**, 76 (1985).
- <sup>30</sup>P. H. Poole, U. Essmann, F. Sciortino, and H. E. Stanley, *Phys. Rev. E* **48**, 4605 (1993).
- <sup>31</sup>O. Mishima, *J. Chem. Phys.* **100**, 5910 (1994).